Physica A 194 (1993) 288–297
North-Holland

PHYSICA A

Multifractal fluctuations in the dynamics of disordered systems

S. Havlin[a,b], A. Bunde[c], E. Eisenberg[a], J. Lee[b], H.E. Roman[c], S. Schwarzer[b] and H.E. Stanley[b]

[a]*Department of Physics, Bar-Ilan University, Ramat-Gan, Israel*
[b]*Center For Polymer Studies and Department of Physics, Boston University, Boston, MA 02215, USA*
[c]*I. Institut für Theoretische Physik, Universität Hamburg, W-2000 Hamburg 36, Germany*

We review recent developments in the study of the multifractal properties of dynamical processes in disordered systems. In particular, we discuss the multifractality of the growth probabilities of DLA clusters and of the probability density for random walks on random fractals. The results for multifractality in DLA are based mainly on numerical studies, while the results for random walks on random fractals are based on analytical results. We find that although a phase transition in the multifractal spectrum occurs for $d = 2$ DLA, there seems to be no phase transition for $d = 3$ DLA. This might be explained by the topological differences between $d = 2$ and $d = 3$ DLA clusters. For the probability density of random walks on random fractals, it is found that multifractality occurs for a finite range of moments q, $q_{\min} < q < q_{\max}$. The approach can be applied to other dynamical processes, such as fractons or tracer concentration in stratified media.

1. Introduction

In recent years it has been demonstrated that for a wide range of dynamical processes in random media the usual scaling laws fail to hold. Instead, quantities describing these processes have anomalously broad distributions characterized by the concept of multifractality [1–10]. The moments of such physical quantities cannot be described by a single exponent. Rather, an infinite hierarchy of exponents is needed to describe them. Some examples are the growth probabilities of diffusion limited aggregation (DLA) [3–6], the voltage drops in percolation clusters [7], the probability density of random walks on fractals [8], the tracer concentration in stratified media with random fields [9], and the amplitudes of vibrational excitations [10], called fractons, in percolation systems.

In this review we concentrate on recent developments in two examples. One is the DLA in which the multifractality finding is based on numerical simula-

Elsevier Science Publishers B.V.

tions and the other is multifractality of the probability density of random walks on random fractals for which an analytical approach exists.

2. Diffusion-limited aggregation (DLA)

The diffusion-limited aggregation model [11] is found to describe a wealth of diverse physical, chemical and biological phenomena [3]. The dynamical growth process of DLA is characterized by the set of growth probabilities $\{p_i\}$, where $p_i \equiv p_i(M)$ is the probability that site i in a cluster of mass M will be the next to grow. The set $\{p_i\}$ for a given cluster describes the statistical scaling properties of the growth of the cluster. A useful approach to describe the statistical properties of the DLA growth is the multifractal formalism. First, one calculates the "partition function" defined as the qth moment of the distribution of p_i,

$$Z(q, M) \equiv \left\langle \sum_{i=1}^{M} p_i^q \right\rangle . \tag{1}$$

The average $\langle \ldots \rangle$ is over different clusters with mass M. The effective scaling exponent $\tau(q, M)$ is defined to be

$$\tau(q, M) \equiv -\partial \ln Z(q, M) / \partial \ln M . \tag{2}$$

If the asymptotic limit

$$\tau(q) \equiv \lim_{M \to \infty} \tau(q, M) \tag{3}$$

exists, then $\tau(q)$ characterizes the power-law scaling of $Z(q, M)$ as a function of M, i.e.,

$$Z(q, M) \sim M^{-\tau(q)} . \tag{4}$$

The multifractal spectrum $f(\alpha)$ is obtained by the Legendre-transformation of $\tau(q)$,

$$f(\alpha) \equiv q\alpha - \tau(q) , \qquad \alpha \equiv \frac{\mathrm{d}\tau(q)}{\mathrm{d}q} . \tag{5}$$

If $\tau(q)$ is linear in q then the system is uni-fractal, i.e., it is characterized by a single exponent. However, if $\tau(q)$ is non-linear in q, the system is called multifractal. In the "thermodynamic formalism" $\tau(q)$ corresponds to a "free energy". If for some range of q values, e.g., for $q < q_c$, $Z(q, M)$ does not scale

as a power law of M (as in eq. (4)), but decays faster, then this implies that $\tau(q, M)$ diverges; we call this phenomenon a "phase transition" at $q = q_c$ [6, 12–14].

The multifractal spectrum, $f(\alpha)$, has been studied extensively for 2D DLA [12–14]. The effectively scaling exponent $\tau(q, M)$ was found numerically to diverge with M for moments $q < q_c \approx 0$, indicating a phase transition. In particular the numerical data suggest [14] that the typical smallest growth probability, $p_{\min}$, does not scale as a power of M, rather as $p_{\min} \sim \exp(-\text{const} \times \ln^2 M)$ [14].

In a recent numerical study [15], the distribution $n(\alpha, M)$ has been calculated. Here $\alpha \equiv -\ln p / \ln M$ and $n(\alpha, M)\,\mathrm{d}\alpha$ is the number of growth sites in the cluster of mass M with α-values between α and $\alpha + \mathrm{d}\alpha$. It can be easily seen that

$$f(\alpha) \equiv \lim_{M \to \infty} \frac{\ln n(\alpha, M)}{\ln M} . \tag{6}$$

Schwarzer et al. [15] have found, using numerical simulations, that

$$n(\alpha, M) \sim n_0 \exp\left(- \frac{A\alpha^{\gamma}}{\ln^{\delta} M} \right) , \tag{7}$$

where $\gamma \approx 2.0 \pm 0.3$ and $\delta \approx 1.3 \pm 0.3$. Eq. (7) and the form of $p_{\min}$ suggest that we can picture the structure of 2D DLA as composed of hierarchical self-similar "almost voids" connected by narrow "necks". Schwarzer et al. [16] calculated the distribution of voids and necks and found that many very large voids have very narrow necks, supporting the above picture (see fig. 1). Lee et al. [17] have suggested a family of deterministic hierarchical fractals, which possess the above properties, as models for the structure of 2D DLA clusters (see fig. 2). The analytical solution for the growth probability distribution of this family is found to have the form of eq. (7) with $\gamma = 2$ and $\delta = 1$. Eq. (7) can also explain the finding [14] that the mass dependence of the smallest growth probability is $p_{\min} \sim \exp(-A \ln^2 M)$.

In a recent work [18], the multifractal spectrum of the growth probability of 3D off-lattice DLA was studied. The results indicate that, in contrast to 2D DLA, there appears to be *no* phase transition in the multifractal spectrum (see fig. 3). In particular, it is found [18] that for 3D DLA $p_{\min} \sim M^{-\alpha_{\max}}$ where $\alpha_{\max} \simeq 4.3 \pm 0.2$. This difference can be explained in terms of the topological differences between 2 and 3 dimensions. In both 2D and 3D, narrow necks are created in the DLA by side branches that grow closer and closer. In this process the growth probabilities in the neck become so small that it does not

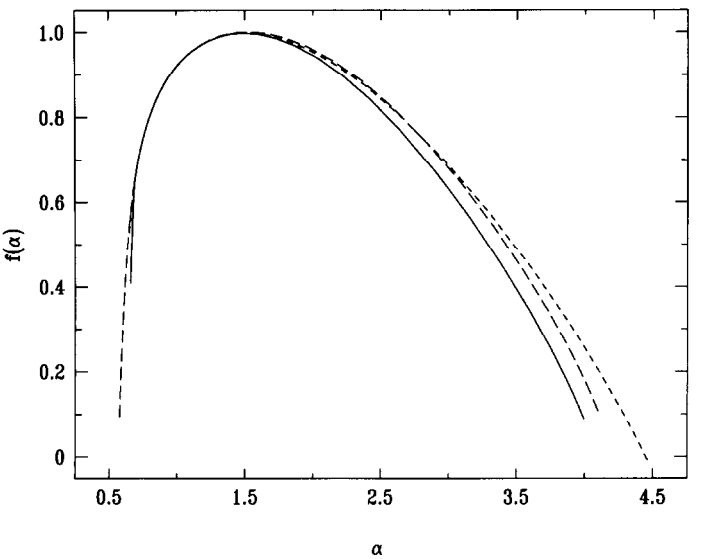

Fig. 1. $f(\alpha)$ vs. $\alpha \equiv \partial\tau(q)/\partial q$, calculated as the Legendre transform of $\tau(q)$ for 3D DLA. $\tau(q)$ is determined from a linear least square fit of the logarithm of the moments $Z(q, M)$ as a function of the logarithm of the DLA cluster mass $\log M$. The largest considered clusters were of mass $M = 15\,015$. Different curves correspond to fits in an increasingly larger mass range: $M = 10\,330$–$15\,015$ (solid line), $M = 7\,502$–$15\,015$ (short dashes) and $M = 2\,892$–$15\,015$ (long dashes).

become narrower. Due to the 2D topology the growth probabilities inside the "almost void" are extremely small. This, together with the hierarchical picture of the DLA, explains the relation $p_{\min} \sim \exp(-\ln^2 M)$, which leads to a phase transition. In 3D, even when tips from different branches are close, there is no significant screening of growth, since particles can enter from directions perpendicular to the loop, suggesting a power-law dependence of $p_{\min}$ on the mass M of the cluster. Thus the apparent absence of a phase transition in 3D DLA can be interpreted as due to the topological difference between 2 and 3 dimensions.

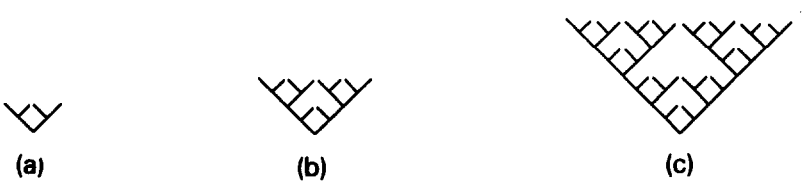

Fig. 2. Construction of a deterministic hierarchical model for DLA. (a) The generator and the first generation of the model; (b) the second generation; and (c) the third generation (after ref. [17]).

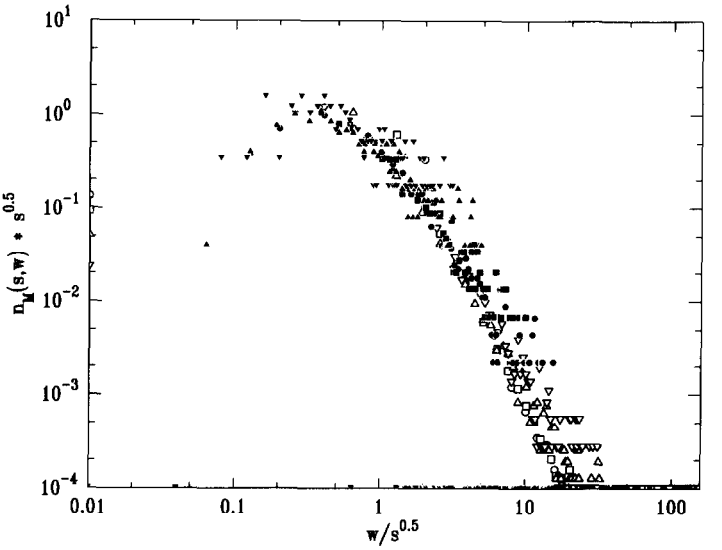

Fig. 3. Neck width distributions in 2D DLA. Here, $n_M(s, w)$ is the normalized number of "almost voids" with size w associated to "voids" of area s, for 21 DLA clusters with $M = 120\,000$ sites. On the abscissa, we plot the rescaled neck width $w/s^{0.5}$. The ordinate is $n_M(s, w)\, s^{0.5}$ to preserve the normalization of the distributions. Displayed are $s = 1$ (○), 3 (□), 10 (△), 25 (▽), 100 (●), 250 (■), 1000 (▲), 2500 (▼). For the large s, a maximum in the distributions is seen, corresponding to a typical value $\tilde{w}(s) \sim s^{0.5}$ of the neck width. Note, however, that this value is small ($\approx$10 for $s = 2500$).

3. Multifractal fluctuations of random walks on random fractals

A random fractal is characterized by two metrics: (i) the geometrical distance, r, between two sites and (ii) the chemical distance (or shortest path), ℓ, between two sites. In general, both distances scale differently. In recent years it has been found that the fluctuations of several dynamical properties on fractals (e.g., the probability density of random walks and the amplitudes of vibrational excitations) are very narrow in the chemical distance metric and very broad – exhibiting multifractal features – in the geometrical distance. Since dynamical processes propagate along the shortest path, the chemical space is a more natural metric for dynamics.

To demonstrate the above differences, notice that the probability density $P(\ell, t)$ of a random walker on a linear fractal at chemical distance ℓ and at time t is *identical* for any configuration of the linear fractal, i.e., there are zero fluctuations. However, when calculating $P(r, t)$, the probability of finding a random walker at distance r on a linear fractal will have very different values for different configurations. The multifractal features of $P(r, t)$ can be demonstrated rigorously for random walks on linear fractals [19, 20]. Here we review

results for random walks on more general random fractals including the physically interesting case, percolation clusters.

As has been recently demonstrated [8, 19], the fluctuations of $P(r, t)$ on fractals display multifractal features characterized by a non-standard behavior of the moments $\langle P^q(r, t)\rangle$ $(q > 0)$, and by an anomalously broad distribution, $N(\log P)$, of the values $P \equiv P(r, t)$ between $\log P$ and $\log P + \mathrm{d} \log P$. We also find [20] that the multifractality exists only for moments q between

$$\left(\frac{t}{r^{d_w}}\right)^{1/(d_w^{\ell}-1)} = q_{\min} < q < q_{\max} = \left(\frac{t}{r}\right)^{1/(d_w^{\ell}-1)} \tag{8}$$

Here, d_w and d_w^{ℓ} are the anomalous diffusion exponents describing the behavior of the mean-square displacement of the random walk in geometrical distance, $R \equiv \sqrt{\langle r^2\rangle} \sim t^{1/d_w}$, and in chemical distance $\langle \ell \rangle \sim t^{1/d_w^{\ell}}$.

To show this, we follow refs. [8, 20] and start with the definition of the configurational average

$$\langle P^q(r, t)\rangle \equiv \frac{1}{N_r} \sum_{i=1}^{N_r} P_i^q(r, t)\,, \tag{9}$$

where the sum is over all N_r sites i of the fractal located a distance r from the origin, and $P_i(r, t)$ denotes the probability to be at site i. Note that N_r includes a very large number of sites.

After time t, the random walk can be at many different sites i at distance r from the origin, and their corresponding probabilities $P_i(r, t)$ may obtain very different values. The crucial point is that the probability to be at the chemical distance ℓ has a narrow distribution [8, 19] for different configurations. Asymptotically, for $\ell/t^{1/d_w^{\ell}} \gg 1$, $P(\ell, t)$ can be approximated to be

$$P(\ell, t) \sim t^{-d_s/2} \exp[-(\ell/t^{1/d_w^{\ell}})^{\delta_\ell}]\,, \qquad \delta_\ell \equiv d_w^{\ell}/(d_w^{\ell} - 1)\,, \tag{10}$$

when $\ell < t$, and $P(\ell, t) = 0$ when $\ell > t$ [#1]. Thus, the sum in (9) can be written as a sum over sites having the same ℓ values,

$$\langle P^q(r, t)\rangle = \sum_{\ell} \left(\frac{N_\ell}{N_r}\right) P^q(\ell, t)\,, \tag{11}$$

where N_ℓ denotes the number of those sites which are at chemical distance ℓ from the origin. Since $P(\ell, t)$ has a narrow distribution, its average moments are assumed to be $P^q(\ell, t)$.

By definition, $N_\ell/N_r \equiv \phi(\ell|r)$ is the probability that two sites separated a distance r are at chemical distance ℓ. Transforming the sum (11) into an

[#1] Here d_s is the fracton dimension [23].

integral over ℓ yields

$$\langle P^q(r,t)\rangle = \int_r^t \mathrm{d}\ell\ \phi(\ell|r)\ P^q(\ell,t)\,. \tag{12}$$

The lower integration limit $\ell = r$ is due to the fact that $\phi(\ell|r) = 0$ when $\ell < r$, while the upper limit comes from the condition that $P(\ell, t) = 0$ when $\ell > t$.

For general random fractals, the structural function ϕ is expected to have the form [21]

$$\phi(\ell|r) \sim \ell^{-1}(r/\ell^{\tilde{\nu}})^g \exp[-a(r/\ell^{\tilde{\nu}})]^{\delta}\,, \qquad \delta \equiv (1-\tilde{\nu})^{-1}\,, \quad \ell > r\,, \tag{13}$$

which satisfies the normalization condition $\Sigma_\ell N_\ell/N_r = 1$, which follows from (11) when $q = 0$. We begin by considering the large time case, $t > r^{d_w}$, where the upper integration limit $\ell = t$ in (12) corresponds to values of ℓ above the maximum of $\phi(\ell|r)$ at $\ell \sim r^{1/\tilde{\nu}}$ ($\tilde{\nu} = d_\ell/d_f$). According to (13), $\phi(\ell|r)$ increases as $\exp[-a(r/\ell^{\tilde{\nu}})^{\delta}]$ for $r < \ell < r^{1/\tilde{\nu}}$, and decreases as $1/\ell^{1+\tilde{\nu}g}$ for $\ell > r^{1/\tilde{\nu}}$.

To evaluate the integral (12), we use the method of steepest descent. The saddle point occurs at

$$\ell = \ell_0 = \left(\frac{r^{1/(1-\tilde{\nu})} t^{\delta_\ell/d_w^\ell}}{q}\right)^{1/[\delta_\ell + \tilde{\nu}/(1-\tilde{\nu})]}\,, \tag{14}$$

which yields

$$\langle P^q(r,t)\rangle \sim \langle P(r,t)\rangle^{q^\gamma} \sim t^{-d_s q/2} \exp\left[-\text{const} \times q^\gamma \left(\frac{r}{R}\right)^u\right], \tag{15a}$$

with

$$\gamma \equiv \frac{d_w^\ell - 1}{d_w - 1} \quad \text{and} \quad u \equiv \frac{d_w}{d_w - 1}\,. \tag{15b}$$

The non-linear q-dependence of the exponent in (15a) shows multifractal behavior for the moments in r-space as discussed in ref. [8].

The fluctuations of $P(r, t)$ can be described by the histogram $N(\ln P)$ giving the number of sites with values $P \equiv P(r, t)$ between $\ln P$ and $\ln P + \mathrm{d}\ln P$. The histogram $N(\ln P)$ is found [8] to be anomalously broad and is given by

$$N(\ln P) \sim [\ln(P/P_0)]^{-\alpha} \exp\left(\frac{-b}{[\ln(P/P_0)]^{\beta}}\right), \qquad P_0 \equiv P(0,t)\,, \tag{16}$$

where $\alpha = [g\tilde{\nu}(d_w^\ell - 1) + 1]/d_w^\ell$ and $\beta = (d_w^\ell - 1)/(d_w - d_w^\ell)$; see also fig. 4.

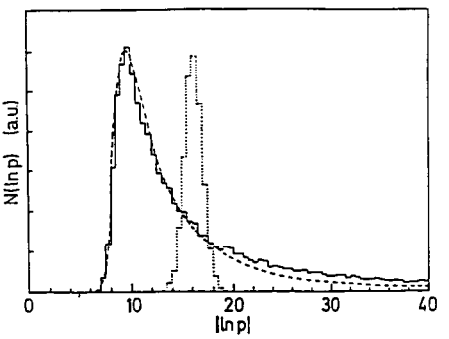

Fig. 4. Representative plot of the histogram $N(\ln P)$ versus $|\ln P|$ for fixed r and t (solid line) and for fixed ℓ and t (dotted line), with $t = 1000$, $r = 30$, and $\ell = 80$. The dashed line represents the theoretical result (16). The narrow histogram in ℓ-space supports the assumption $\langle P^q(\ell, t)\rangle = \langle P(\ell, t)\rangle^q$ made in eq. (12) (after ref. [8]).

The results (15) and (16) are valid only for $r < \ell_0 < r^{1/\tilde{\nu}}$, which yields the range of moments for which multifractality is expected to be valid, eq. (1). For values of q outside the range given by (1), the form of $\langle P^q(r, t)\rangle$ will depend on the form of $\langle P(\ell, t)\rangle$. A reasonable assumption, indirectly supported by numerical simulations on the Sierpiński gasket [22], suggests that $\langle P(\ell, t)\rangle$ for $t \gg \ell^{d_w^\ell}$ has the form $\langle P(\ell, t)\rangle \sim t^{-d_s/2} \exp(-\ell^{d_w^\ell}/t)$. This yields that for $q^{d_w^\ell - 1} r^{d_w}/t \gg 1$ (or $q \ll q_{\min}$), $\langle P^q(r, t)\rangle$ has the form

$$\langle P^q(r, t)\rangle \sim t^{-d_s q/2} \phi(r^{1/\tilde{\nu}}|r) \exp\left(-\text{const} \times q \frac{r^{d_w}}{t}\right). \tag{17}$$

Thus one obtains for $q = 1$

$$\langle P(r, t)\rangle \sim t^{-d_s/2} \exp\left(-\text{const} \times \frac{r^{d_w}}{t}\right), \qquad r \ll t^{1/d_w}, \tag{18a}$$

compared with

$$\langle P(r, t)\rangle \sim t^{-d_s/2} \exp\left[-\text{const} \times \left(\frac{r}{t^{1/d_w}}\right)^{\delta}\right], \qquad r \gg t^{1/d_w}, \tag{18b}$$

obtained from (15a). Recent numerical studies on the Sierpiński gasket [22] are consistent with the crossover of eqs. (18).

For the analogous vibrational excitations on the infinite percolation cluster, called fractons [23], Bunde et al. [10] find that the vibrational amplitude of frequency w, $\psi_i(r, w)$, of sites i at distance r from the center of a typical fracton are characterized by a multifractal spectrum. The q moments of the amplitude

of a fracton are

$$\psi_q(r, w) \equiv \langle \psi^q(r, t) \rangle \sim \exp(-qr/\tilde{\lambda}_q) ,$$

where $\tilde{\lambda}_q \equiv q^{1-d_\ell/d_f}\lambda_1$. Using similar arguments leading to (8) yields the lower cutoff $q_{\min}$ for the multifractal to be

$$q \gg q_{\min} = \frac{\lambda_1}{r^{1/\tilde{\nu}} c^{(1-\tilde{\nu})/\tilde{\nu}}} . \tag{19}$$

Analogous arguments leading to (17) yield

$$\psi_q(r, w) \sim \exp\left(-\frac{qr^{d_{\min}}}{\lambda_1}\right) , \qquad qr^{d_{\min}}/\lambda_1 \ll 1 . \tag{20}$$

Finally, a similar approach leading to eqs. (15) and (16) has been applied [9] to study the fluctuations in tracer concentration when diffusion occurs in a stratified medium. In this model the drift velocities have been assumed to be constant along the x-direction, but varying randomly from layer to layer in the y-direction. This system has been used to model transport of underground water in stratified media [24]. It is found [9] that the fluctuation of the tracer concentration, $P \equiv P(x, t)$, are described by an anomalously broad histogram of the form of eq. (16) with $\alpha = 3$ and $\beta = 2$ (see fig. 5). Moreover, the relative fluctuations $\delta P/P$ increase exponentially with x.

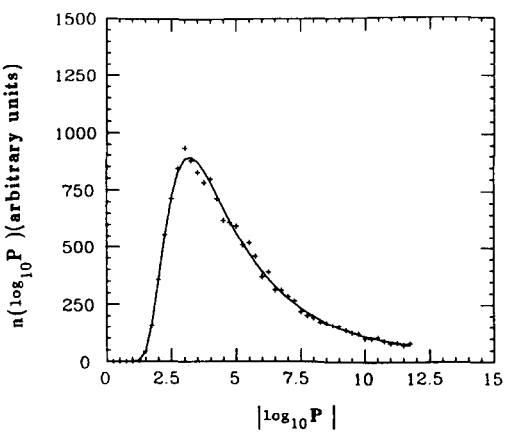

Fig. 5. Histogram $n(\log_{10}P)$ for $u \equiv x/t^{3/4} = 1.47$. The continuous line corresponds to the prediction of eq. (16) with $\alpha = 3$ and $\beta = 2$, and the + symbols to the numerical calculations (after ref. [9]).

Acknowledgements

We are grateful to A. Aharony, M. Araujo, A.B. Harris, P. Meakin and S. Russ for discussions, and to NSF, ONR and DFG for financial support.

References

[1] B.B. Mandelbrot, J. Fluid Mech. 62 (1974) 331.
[2] G. Paladin and A. Vulpiani, Phys. Rep. 156 (1987) 147.
[3] H.E. Stanley, in: Fractals and Disordered Systems, A. Bunde and S. Havlin, eds. (Springer, Heidelberg, 1991) p. 1; H.E. Stanley and P. Meakin, Nature 335 (1988) 405.
[4] T. Vicsek, Fractal Growth Phenomena (World Scientific, Singapore, 1989).
[5] P. Meakin, in: Phase Transitions and Critical Phenomena, vol. 12, C. Domb and J.L. Lebowitz, eds. (Academic Press, Orlando, 1988).
[6] P. Meakin, H.E. Stanley, A. Coniglio and T.A. Witten, Phys. Rev. A 32 (1985) 2364; P. Meakin, A. Coniglio, H.E. Stanley and T.A. Witten, Phys. Rev. A 34 (1986) 3325; C. Amitrano, A. Coniglio and F. di Liberto, Phys. Rev. Lett. 57 (1986) 1016.
[7] L. de Arcangelis, S. Redner and A. Coniglio, Phys. Rev. B 31 (1985) 4725.
[8] A. Bunde, S. Havlin and H.E. Roman, Phys. Rev. A 42 (1990) 6274; S. Havlin and A. Bunde, Physica D 38 (1989) 184.
[9] M. Araujo, S. Havlin and H.E. Stanley, Phys. Rev. A 44 (1991) 6913.
[10] A. Bunde, H.E. Roman, S. Russ, A. Aharony and A.B. Harris (1992) preprint.
[11] T.A. Witten and L. Sander, Phys. Rev. Lett. 47 (1981) 1400.
[12] J. Lee and H.E. Stanley, Phys. Rev. Lett. 61 (1988) 2945; J. Lee, P. Alstrøm and H.E. Stanley, Phys. Rev. A 39 (1989) 6545.
[13] R. Blumenfeld and A. Aharony, Phys. Rev. Lett. 62 (1989) 2977; J. Lee, P. Alstrøm and H.E. Stanley, Phys. Rev. Lett. 62 (1989) 3013.
[14] S. Schwarzer, J. Lee, A. Bunde, S. Havlin, H.E. Roman and H.E. Stanley, Phys. Rev. Lett. 65 (1990) 603.
[15] S. Schwarzer, J. Lee, S. Havlin, H.E. Stanley and P. Meakin, Phys. Rev. A 43 (1991) 1134.
[16] S. Schwarzer, S. Havlin and H.E. Stanley, Physica A 191 (1992) 117.
[17] J. Lee, S. Havlin and H.E. Stanley, Phys. Rev. A 45 (1992) 1035; J. Lee, S. Havlin, H.E. Stanley and J.E. Kiefer, Phys. Rev. A 42 (1990) 4832.
[18] S. Schwarzer, M. Wolf, S. Havlin, P. Meakin and H.E. Stanley, Phys. Rev. A 46 (1992) R3016.
[19] A. Bunde and S. Havlin, eds., Fractals and Disordered Systems (Springer, Heidelberg, 1991).
[20] E. Eisenberg, A. Bunde, S. Havlin and H.E. Roman, Phys. Rev. A, in press.
[21] U.A. Newman and S. Havlin, J. Stat. Phys. 52 (1988) 203; and to be published.
[22] J. Klafter, G. Zumofen and A. Blumen, J. Phys. A 24 (1991) 4835; S. Havlin, R. Nossal, B. Trus and G.H. Weiss, Phys. Rev. A 45 (1992) 7551.
[23] S. Alexander and R. Orbach, J. Phys. Lett. (Paris) 43 (1987) L625.
[24] G. Dagan, J. Fluid. Mech. 145 (1984) 151; A. Dieulin, G. Matheron and G. de Marsily, in: Flow and Transport in Porous Media (Balkema, Rotterdam, 1981) p. 199; G. Dagan, Annu. Rev. Fluid. Mech. 19 (1987) 183; G. Matheron and G. de Marsily, Water Resour. Res. 16 (1980) 901; R.M. Mazo and C. van den Broeck, J. Chem. Phys. 86 (1987) 450; J.P. Bouchaud, A. Georges, J. Koplik, A. Provata and S. Redner, Phys. Rev. Lett. 64 (1990) 2503; P. Le Doussal and J. Machta, Phys. Rev. B 40 (1989) 2427; G. Zumofen, J. Klafter and A. Blumen, Phys. Rev. A 42 (1990) 4601.